NeuroImage 188 (2019) 584–597

Contents lists available at ScienceDirect

NeuroImage

journal homepage: www.elsevier.com/locate/neuroimage

Dynamics of aesthetic experience are reflected in the default-mode network

Amy M. Belfi [a,*,1], Edward A. Vessel [b,**,1], Aenne Brielmann [c], Ayse Ilkay Isik [b], Anjan Chatterjee [d], Helmut Leder [e], Denis G. Pelli [c], G. Gabrielle Starr [f]

[a] Department of Psychological Science, Missouri University of Science and Technology, Rolla, MO, USA
[b] Department of Neuroscience, Max Planck Institute for Empirical Aesthetics, Frankfurt, Germany
[c] Department of Psychology, New York University, New York, NY, USA
[d] Department of Neurology, University of Pennsylvania School of Medicine, Philadelphia, PA, USA
[e] Department of Basic Psychological Research and Research Methods, University of Vienna, Vienna, Austria
[f] Department of English, Pomona College, Claremont, CA, USA

A B S T R A C T

Neuroaesthetics is a rapidly developing interdisciplinary field of research that aims to understand the neural substrates of aesthetic experience: While understanding aesthetic experience has been an objective of philosophers for centuries, it has only more recently been embraced by neuroscientists. Recent work in neuroaesthetics has revealed that aesthetic experience with static visual art engages visual, reward and default-mode networks. Very little is known about the temporal dynamics of these networks during aesthetic appreciation. Previous behavioral and brain imaging research suggests that critical aspects of aesthetic experience have slow dynamics, taking more than a few seconds, making them amenable to study with fMRI. Here, we identified key aspects of the dynamics of aesthetic experience while viewing art for various durations. In the first few seconds following image onset, activity in the DMN (and high-level visual and reward regions) was greater for very pleasing images; in the DMN this activity counteracted a suppressive effect that grew longer and deeper with increasing image duration. In addition, for very pleasing art, the DMN response returned to baseline in a manner time-locked to image offset. Conversely, for non-pleasing art, the timing of this return to baseline was inconsistent. This differential response in the DMN may therefore reflect the internal dynamics of the participant's state: The participant disengages from art-related processing and returns to stimulus-independent thought. These dynamics suggest that the DMN tracks the internal state of a participant during aesthetic experience.

Neuroaesthetics is a rapidly developing interdisciplinary field of research that aims to understand the neural processes underlying aesthetic experiences (Chatterjee and Vartanian, 2014; Pearce et al., 2016). Several theories describe an aesthetic experience as a series of processing stages, beginning with low-level perceptual analysis and culminating in a judgment or action (Chatterjee, 2004; Leder and Nadal, 2014; Pelowski et al., 2017). A recent investigation of the temporal evolution of aesthetic experience found that aesthetic pleasure evoked by a visual image grows over a few seconds, is sustained, and decays slowly, over one hundred seconds after image offset (Brielmann and Pelli, 2017).

Despite the theoretical and psychophysical characterization of these temporal dynamics, most neuroimaging work has treated aesthetic experience as a static event. For example, viewers are typically asked to make a single binary judgment such as characterizing an artwork as 'beautiful' or 'not beautiful.' Despite the lack of a temporally extended behavioral measurement, this work provides some hints as to the neural dynamics of aesthetic experience. Prior fMRI data suggest two distinct neural systems underlying aesthetic experience: One, consisting primarily of perceptual and reward-related regions, responds in a manner that is linearly related to aesthetic appreciation, while a second, consisting of prefrontal and default mode network (DMN) regions, is only engaged by artwork deemed strongly aesthetically moving by the viewer (Vessel et al., 2012). MEG data suggest one set of brain regions is engaged during initial exposure to an artwork (250–750 ms post-onset), while a second set of regions, whose pattern is consistent with the DMN, is active during a later time window (1000–1500 ms; Cela-Conde et al., 2013). This timing is consistent with the fMRI BOLD signal timecourse observed in anterior medial prefrontal cortex (aMPFC), a core node of the DMN, where an initial suppression was followed by a rise several seconds later only for those artworks found most aesthetically appealing (Vessel et al., 2013). Additionally, an fMRI study of facial attractiveness found that reward regions were temporally dissociable during aesthetic preference judgments: The nucleus accumbens was engaged earlier and the orbitofrontal cortex was engaged later (Kim, Adolphs, O'Doherty and Shimojo, 2007). Similar work investigating the neural correlates of creative cognition have identified this as a two-step process, also involving

* Corresponding author. Department of Psychological Science, Missouri S&T, 135 H-SS, Rolla, MO, 65409, USA.
** Corresponding author. Max Planck Institute for Empirical Aesthetics, Grüneburgweg 14, 60322, Frankfurt am Main, Germany.
E-mail addresses: amybelfi@mst.edu (A.M. Belfi), ed.vessel@ae.mpg.de (E.A. Vessel).
[1] These authors contributed equally to this work.

https://doi.org/10.1016/j.neuroimage.2018.12.017
Received 31 July 2018; Received in revised form 26 November 2018; Accepted 9 December 2018
Available online 10 December 2018

engagement of the DMN (for review, see Beaty et al., 2016). Overall, this work identifies at least three large-scale networks involved in aesthetic experience – perceptual, reward, and default-mode networks – and indicates that these networks are differentially engaged during exposure to artworks the viewer finds especially aesthetically appealing.

One major unresolved issue is the potential effects of stimulus duration on the cognitive and neural correlates of aesthetic experience. For example, prior work in museum settings has identified the average looking time as 28–38 s (Brieber et al., 2014), which is substantially longer than most artworks are presented in prior neuroaesthetics research. Recent work investigating aesthetic responses to music has identified that listeners can make accurate aesthetic judgments in as little as hundreds of milliseconds (Belfi et al., 2018a). As recent attention has been dedicated to studying neural responses to extended, naturalistic stimuli, primarily in the auditory domain (Burunat et al., 2014; Desai et al., 2016; Huth et al., 2016), we sought to investigate the neural correlates of aesthetic experience in response to both shorter and extended viewings of artworks. In addition to identifying differences in aesthetic experience to artworks of varying durations, this allows for identification of responses to stimulus *onset* versus stimulus *offset*. There has been evidence for multiple stages of processing during aesthetic experience, some of which may only occur after prolonged exposure to or removal of the visual stimulus (Cela-Conde et al., 2013; Jacobsen and Höfel, 2003). Yet, these differential responses to stimulus onset and offset versus stages of aesthetic experiences have not yet been characterized neurally. Therefore, it is unknown which neural responses correspond to the initial and later stages of aesthetic experience, versus those that correspond to stimulus onset/offset.

An additional unresolved issue, when looking at more naturalistic viewing times, is the issue of extended behavioral responses to aesthetic experiences. In standard aesthetics experiments, participants view an aesthetic object and are asked to make a discrete, summative rating about that object. For example, viewers often make a binary judgment such as characterizing an artwork as 'beautiful' vs. 'not beautiful' (Cela-Conde et al., 2009, 2013; Flexas et al., 2014; Kornysheva et al., 2010; Müller et al., 2010; Munar et al., 2012). More commonly, aesthetic judgments are made on a discrete Likert-scale, where participants rate an item's degree of beauty or aesthetic appeal (Bohrn et al., 2013; de Tommaso et al., 2008; Jacobs et al., 2012; Jacobsen et al., 2006; Kawabata and Zeki, 2004; Mallon et al., 2014). One disadvantage of this approach is that a summary judgment after a stimulus has been presented gives no insight into experience *during* one's engagement with the work of art, and substitutes a post-hoc measure for what is fundamentally a dynamic experience.

Research in other fields has taken a moment-based, continuous approach to record behavioral responses dynamically during stimulus presentation. In fact, research from other fields has indicated that a post-stimulus summary judgment may not accurately reflect the moment-by-moment experience during the stimulus (Do et al., 2008; Kahneman, 2000b). Various metrics of the continuous trace, such as the mean, peak value, maximum slope, or end value, have been used to predict an overall rating, with varying degrees of success (Rozin et al., 2004; Schafer et al., 2014). Overall, this research indicates that overall and continuous measurements capture different aspects of an experience. Given this disparity, the application of continuous methods to the field of neuroaesthetics is necessary to understand the temporal dynamics of aesthetic experience.

In the present work, we varied the duration of the stimulus presentation and continuously measured behavioral and neural responses during a 14 s post-stimulus period. We aimed to identify: 1) which brain networks respond differentially to aesthetic appreciation, 2) when this response occurs, and 3) which aspects of the response are tied to stimulus onset and offset. We predicted that 1) regions in the DMN would be suppressed during image presentation, 2) DMN signal during highly-pleasing artworks would show a reduction or even reversal of this stimulus-related suppression, and that 3) DMN activity would show a 'lingering' of increased activity during the post-stimulus period, similar to the behavioral evidence for sustained aesthetic appreciation. Conversely, we predicted that reward-related regions and higher-level visual regions would be affected by aesthetic appreciation during stimulus exposure but that this would not persist after image offset.

1. Materials and methods

1.1. Participants

Thirty participants were recruited at New York University and paid for their participation. Five participants were excluded due to excessive motion (see below), leaving a final group of 25 participants (8 men, 17 women; 24 right-handed; 27.56 ± 6.49 years of age). The Institutional Review Board approved this study and all participants gave informed consent in accordance with the New York University Committee on Activities Involving Human Subjects.

Our sample size was determined by conducting a power analysis based on data from our previous work, which reported effect sizes in DMN regions of interest (ROIs) around $\eta^2 = 0.80$ (Vessel et al., 2012). Using G*Power software (Faul et al., 2007), this power analysis indicated a sample of 20 participants would be sufficiently powerful (at a 1-β level of 0.95) to detect an effect this large. Thus, our sample size is more than adequate for the main objective of this study and should allow for sufficient power to detect our predicted effects.

1.2. Stimuli

Images selected were chosen from those used in previous work (Vessel et al., 2012). Ninety images were selected from the Catalog of Art Museum Images Online database (CAMIO: http://www.oclc.org/camio). These images are high-quality photographs of paintings from a variety of cultural traditions (American, Asian, European) and time periods (15th century to the present). Commonly reproduced images were not included in order to minimize familiarity; in a previous study using more images (109 artworks; Vessel et al., 2012), very few participants (four of sixteen), some of whom had extensive art history expertise, were able to identify specific artworks that had been seen previously, though a larger number (eleven) expressed vague familiarity with "a few" images. Images were scaled so that the largest dimension did not exceed 20° of visual angle and the area did not exceed 75% of a 20° box. Stimulus presentation was controlled using the Psychophysics Toolbox in MATLAB (Brainard, 1997; Pelli, 1997). See Fig. 1A for examples of the stimuli used.

1.3. Procedure

Prior to the experiment, participants completed a brief (~10 min) training session using images not presented in the experiment to familiarize themselves with the task and response modalities. This training session was identical to the experimental procedures, such that participants were not given visual feedback when using the squeezeball. Before beginning the experiment, participants were debriefed to ensure they were comfortable using the squeezeball as a response modality.

During the fMRI experiment, participants viewed the 90 stimuli for one of three durations: 1, 5, or 15 s. In order to capture participants' initial response to each artwork, and since aesthetic appreciation may change based on prior exposure (Cutting, 2003; Park et al., 2010), each stimulus was presented only once over the course of the experiment. Therefore, participants saw 30 stimuli per duration. Image presentation was counterbalanced across participants, across durations, such that each image appeared a roughly equal number of times in each duration.

Each trial began with a 1 s blinking fixation cross, followed by an image of an artwork. At the onset of the image, participants began continuously rating the pleasure they felt from the stimulus (Fig. 1A). Exact instructions to the participants were as follows: "When the image

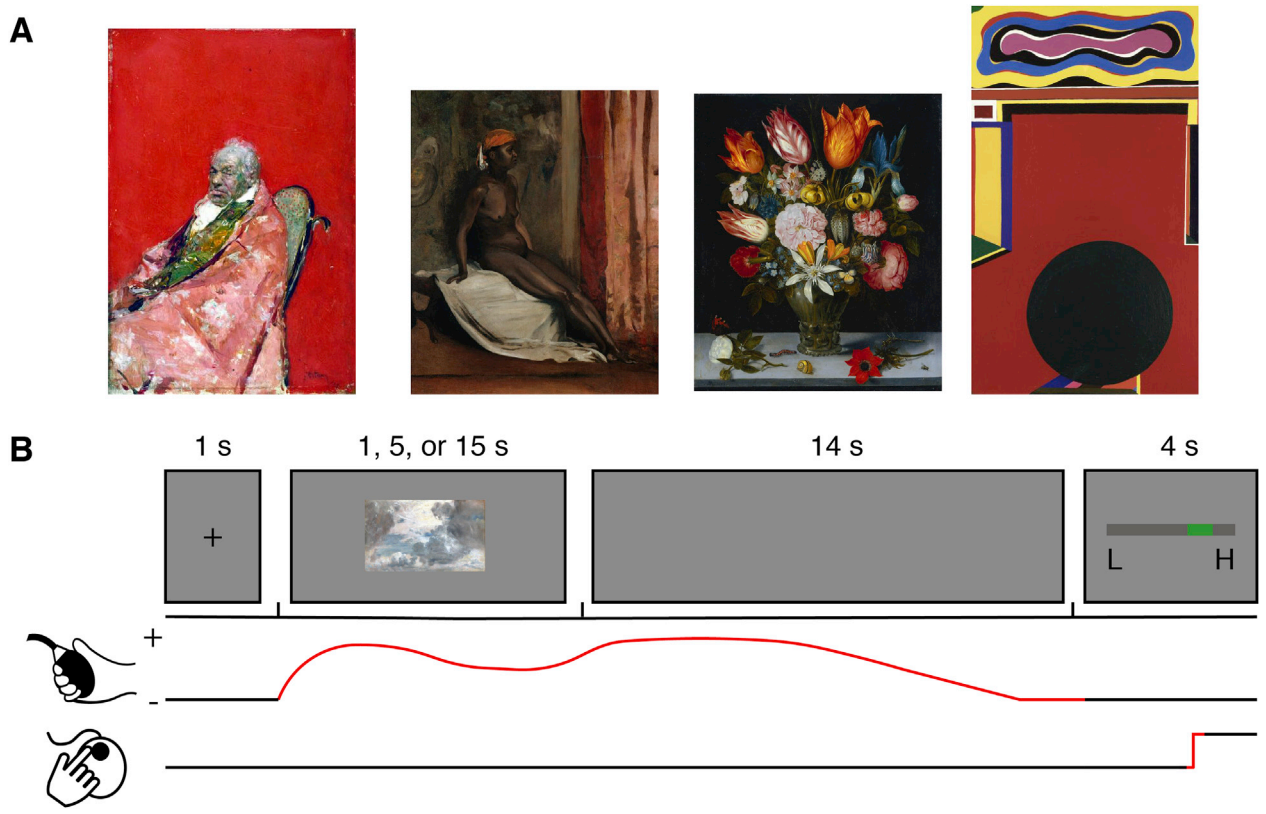

Fig. 1. Stimuli and trial structure. A. Examples of stimuli. See *Acknowledgments* for image credits. **B.** Depiction of trial structure. Trials consisted of a 1 s fixation cross, followed by stimulus presentation for either 1, 5, or 15 s. At stimulus onset, participants began continuously rating their pleasure using an fMRI-compatible squeezeball. After stimulus offset, participants continued rating their pleasure during a 14 s post-stimulus period. Following this post-stimulus period, participants had 4 s to make an overall rating of the stimulus between low (L) and high (H) using a track ball held in the opposite hand.

appears on the screen, begin rating the pleasure you experience from the image" (full instructions can be found in the *Supplementary Materials*). These continuous measurements were recorded using an fMRI-compatible squeeze-ball and sampled at a rate of 10 Hz. The squeeze-ball was used to provide haptic feedback, so participants were aware of their rating without the need for visual feedback (Nielsen, 1987). Participants were not aware of the duration of the stimulus prior to stimulus presentation. Following stimulus presentation, the screen remained blank for a 14 s 'post-stimulus' rating period during which the participants continued to rate the pleasure they were experiencing from having seen the artwork. After this post-stimulus rating period, a visual slider bar appeared on the screen and participants used a trackball in their opposite hand to make a single rating of their 'overall' aesthetic appreciation of the image (4 s max response window). The instructions given to the participant stated: "Please rate, overall, how much this image 'moved' you. That is, how powerful, pleasing, or profound did you find the image." See Fig. 1B for a visual depiction of the trial structure.

1.4. fMRI scanning procedures

All fMRI scans took place at the NYU Center for Brain Imaging (CBI) using a 3T Siemens Allegra scanner with a Nova Medical head coil (NM011 head transmit coil). Stimuli were presented using back-projection onto a screen mounted in the scanner and viewed through a mirror on the head coil.

The 90 artworks were divided into five runs and presented in an event-related design, with each run containing 6 trials of each duration. Timing of stimulus onset, ordering of 1, 5, and 15 s trials, and inter-trial-intervals (mean ITI = 6.76 s, range = 2–20 s) were calculated using the OptSeq2 Toolbox (https://surfer.nmr.mgh.harvard.edu/optseq). Whole-brain BOLD signal was measured from thirty-four 3 mm slices using a custom multi-echo (ME) echo-planar imaging (EPI) sequence (2 s TR, 80 × 64 3 mm voxels, right-to-left phase encoding, FA = 75°). The ME EPI sequence and a tilted slice prescription (15–20° tilt relative to the AC-PC line) were used to minimize dropout near the orbital sinuses. We collected a custom calibration scan to aid in ME reconstruction, unwarping and alignment. Prior to the experimental runs, participants completed a 6-min eyes-open rest scan. Following the functional scans, participants completed a high-resolution (1 mm^3) anatomical scan (T1 MPRage).

1.5. Experimental design and statistical analysis

1.5.1. Behavioral data preprocessing

1.5.1.1. Continuous rating. The continuous rating data underwent a series of preprocessing steps prior to analysis. Due to the mechanics of the squeezeball used to acquire the continuous data, a high-frequency 'spike' often accompanied the onset of each squeeze. To remove these artifacts and other high-frequency noise, a low-pass filter (cutoff frequency 0.25 Hz) was applied to the continuous rating data. Each run was then normalized by scaling the continuous rating data based on the average of two 'maximum' squeezes provided by the participant prior to the start of each run. Participants were instructed to make these maximum squeezes correspond to their maximum rating, not the hardest they could possibly squeeze. They were instructed to pick a level that could be sustained throughout the course of the experiment. All continuous data were scaled in this way for each run for each participant, so continuous data for all participants ranged between 0 and 1.

1.5.1.2. Overall rating. Each overall rating was a single value ranging between 0 and 1. Trials were designated as 'high,' 'medium,' and 'low'

aesthetic appreciation based on the value of the overall rating given at the end of each trial. This binning into 'high,' 'medium,' and 'low' was done separately for each individual participant, not across all trials. Overall, participants tended to use the entire range of the scale when making their responses (see Fig. S2 for an illustration of the range of participants' ratings). Within each duration level (1, 5, 15 s), trials were divided into thirds, and the top third was designated as being high, the middle third as medium, and the bottom third as low. This *post-hoc* trial categorization resulted in nine total trial types: Three durations (1, 5, and 15 s) and three rating-levels (low, medium, and high), with ten trials in each of the nine types. These trial types were used for analysis of both the behavioral and fMRI data.

1.5.2. Behavioral data analysis

Continuous pleasure ratings are well fit by a simple model adapted from previous studies (Brielmann & Pelli, 2017; Brielmann et al., 2017). To assess how pleasure amplitude, as identified by this model, changes with rating-level and stimulus duration, we conducted a 3×3 repeated measures ANOVA.

1.5.3. fMRI preprocessing

ME EPI images were reconstructed using a custom algorithm designed by the NYU Center for Brain Imaging to minimize dropout and distortion, and were tested for data quality (e.g. spikes, changes in signal-to-noise) using custom scripts. The scans were then preprocessed using the FMRIB Software Library (FSL; Oxford, UK) to correct for motion, align data across scans and apply a high-pass filter (0.01 Hz cutoff). High resolution anatomical scans were segmented using FreeSurfer (http://surfer.nmr.mgh.harvard.edu).

A measure of framewise movement displacement (*fmd*) was calculated from the estimated translational movements (*x, y z*) as:

$$fmd_n = t_n - t_{n-1}$$

$$t_n = \sqrt{x_n^2 + y_n^2 + z_n^2}$$

This measure is similar to the framewise displacement (Power et al., 2012) but simpler to compute. Inspection of the maximum *fmd* for each participant revealed four clear outliers (see Fig. S1 in *Supplementary Materials*). Data from these participants was not used for subsequent processing. Data from one additional participant was also removed; this participant moved after the initial localizer scan, bringing a large portion of their brain out of the circle of homogenous signal.

1.5.4. ROI selection and analysis

Three network ROIs were selected based on our *a priori* hypotheses regarding visual, reward, and DMN networks. Additionally, the frontoparietal control network (FP), an important network for goal-directed cognition (Spreng et al., 2010), was analyzed for comparison (included in the *Supplementary Materials*). We selected ROIs in one of two ways. For the DMN, visual and FP network ROIs, we used the rest scan to functionally localize these networks in individual participants. After preprocessing (motion correction, high-pass filtering at 0.005 Hz, spatial smoothing with 6 mm FWHM Gaussian filter), independent component analysis (ICA) was performed on individual participants' scans using MELODIC (FSL). MELODIC determines the appropriate size of the lower-dimensional space using the Laplace approximation to the Bayesian evidence of the model order (Beckmann et al., 2001; Minka, 2000). This process resulted in an average of 24 spatial components (SD = 9.5) for each participant. These ICA components were then moved into MNI standard space and compared to a set of pre-defined network maps (Smith et al., 2009) using Pearson correlation. The component with the highest correlation to the Smith et al. (2009) DMN map was then visually inspected to ensure that its spatial distribution appeared similar to the canonical DMN. For six participants, the DMN was split between two ICA components, which were combined to form a single component. The final DMN ROI for each participant was then defined as the voxels from this component that also belonged to gray matter (as defined by the FreeSurfer gray matter segmentation).

After transformation of these volumetric DMN maps to cortical surface space, a set of five subregions (anterior medial prefrontal cortex, aMPFC; dorsal medial prefrontal cortex, dMPFC; ventral medial prefrontal cortex, vMPFC; posterior cingulate cortex, PCC; inferior parietal lobule, IPL) were identified in each hemisphere by masking the DMN map with a set of "master" ROIs delineated on the Freesurfer fsaverage brain. These master ROIs, which each covered a contiguous region of cortex larger than the corresponding DMN subregion in any one participant, were drawn from the distribution of locations of these subregions observed in an independent sample of 16 participants. This method was used in order to identify previously characterized, spatially specific nodes of the DMN from each individual's own functional connectivity in a manner that required minimal manual intervention. For the higher-level visual network, the component with the highest correlation to the Smith et al. (2009) "lateral visual" network was used, and the ROI was created in the same manner as the DMN. More specifically, we selected the "lateral visual" network since the inferior temporal sulcus (ITS; MNI coordinates -49 -61 -2) activation reported in Vessel et al. (2012) falls within this network mask. For the FP network, the components with highest correlation to Smith et al. (2009) "left frontoparietal" and "right frontoparietal" networks were identified. Eleven participants had a single bilateral component, twelve had two lateralized components that were combined, and two had no acceptable match, leaving 23 participants for FP. Basal ganglia ROIs were defined anatomically based on the FreeSurfer "aparc" automatic segmentation. The caudate, putamen, pallidum, and nucleus accumbens were individually identified (bilaterally) and then combined to form the whole basal ganglia ROI.

General linear modeling was implemented using custom software written in MATLAB (MathWorks; Natick, MA, USA). Following extraction of an average timeseries from each ROI, residual signal variation due to head motion was removed by projecting out the framewise displacement vector and its absolute value. Since the post-hoc trial sorting (by overall rating) resulted in an unequal number of trials in each condition per scan, the timecourses from all five scans were z-scored and concatenated. This ROI timecourse was then modeled using a set of finite impulse response (FIR) functions time-locked to stimulus onset, one for each of the nine conditions (3 presentation durations x 3 rating groups). Each FIR included image presentation, the post-stimulus rating period, the overall-response period and 8 trailing timepoints. The resulting parameter estimates were then averaged across participants for each time bin, resulting in estimates of fMRI signal change across the entire trial for each trial type, as well as an estimate of error at each timepoint (standard error of the mean; SEM).

The high-, medium-, and low-rated trial conditions were compared using repeated-measures ANOVA for each ROI at each presentation duration (i.e., 1, 5, 15 s). These ANOVAs were conducted with time (from image onset until end of post-stimulus period) and condition (high, medium, and low) as within-subjects factors (e.g., Shulman et al., 1999). As our goal was to identify at which time points high trials differed from low trials, we sought to identify any time by condition interactions. In this way, we chose to treat the low-rated trials as a "control" condition, as opposed to using a more standard "control" of, say, scrambled visual images. Importantly, including modified images (such as scrambled images) would interfere with the content of the stimuli (Fairhall and Ishai, 2008) which would likely have large effects on the aesthetic appeal of the images. This would then introduce a confound into the experiment, as it is likely that scrambled images would be more likely to fall within the "low-rated" group. Instead, considering the low-rated trials themselves as a neutral "control" preserves the same content across the three categories, as all low-, medium-, and high-rated images are still intact artworks. All interactions are reported and include measures of effect size (η_p^2). Any significant interactions were followed up by tests of simple main effects for pairwise comparisons; all were corrected for multiple

comparisons using Bonferroni correction (all p-values reported are corrected p-values) and include measures of effect size (Cohen's *d*).

2. Results

2.1. Continuous pleasure ratings well fit by a prior model

Continuous pleasure ratings were well fit by a simple model adapted from a previous study using a different manual response (finger spread on the surface of an iPad, eqs. (1)–(4) in Brielmann and Pelli, 2017). The model supposes a stable initial response level $r_{initial}$. After stimulus onset, pleasure asymptotically approaches the steady-state r_{steady} as a decaying exponential with time constant τ_{short}. After stimulus offset, pleasure asymptotically approaches the final response level r_{final} as a function of two decaying exponentials. The first begins shortly after stimulus onset (τ_{short} after onset) and has the same time constant as the initial approach τ_{short}. The second is added to the first and begins at stimulus offset; it has the time constant τ_{long}.

The model has 5 free parameters: $r_{initial}$, r_{steady}, r_{final}, τ_{short}, τ_{long}. The amplitude of the curves representing felt pleasure is denoted by r_{steady}. We fit the model to pleasure responses averaged per participant for each condition (overall rating group [high, medium low] crossed with duration [1, 5, 15 s]) for fitting the model (see Eqs. (1)–(3)). Responses were first averaged before fitting the model, because single-trial responses are too noisy to achieve a robust model fit. We fit all nine curves at once, allowing a different r_{steady} for each curve, and a single value for each of the remaining parameters, minimizing RMS error. The model fit the data well (RMSE = 0.05; see Fig. 2A–C) and had the following parameter values $r_{initial} = 0.00$; $r_{final} = -0.05$; $\tau_{short} = 5.48$ s; $\tau_{long} = 424.91$ s.

As in our prior work (Brielmann and Pelli, 2017; Brielmann et al., 2017), we chose to focus on model fits where all parameters but r_{steady} are fixed. However, here, we also attempted to fit the model by allowing τ_{short} to vary per duration. This does minimize the slight lag of the model fit for the 1 and 5s durations (see Fig. S2), but does not improve RMSE (0.0479). Additionally, the resulting τ_{short} values are not substantially different (4.9, 5.3, and 6.3 s for the 1, 5, and 15 s durations respectively). For reasons of parsimony, we therefore decided to conduct all further analyses using the original model fits, with all fixed parameters except r_{steady}.

$$\widehat{R} = \alpha_{on}(t) r_{initial} + (1 - \alpha_{on}(t))\left[\alpha_{off}(t) r_{steady} + \left(2 - \alpha_{off}(t)\right) r_{final}\right] \quad (1)$$

$$\alpha_{on}(t) = \exp\frac{-\lfloor t - t_{on} \rfloor}{\tau_{short}} \quad (2)$$

$$\alpha_{off}(t) = \exp\frac{-\lfloor t - (t_{on} + \tau_{short}) \rfloor}{\tau_{short}} + \exp\frac{-\lfloor t - t_{off} \rfloor}{\tau_{long}} \quad (3)$$

The parameter r_{steady} can thus be used to summarize the time course of the pleasure response. It is roughly equivalent to the amplitude of the pleasure curve and we will thus refer to r_{steady} here as *pleasure amplitude* for ease of readability. Amplitude was chosen for our analyses here, as opposed to, say, area under the curve, because our prior behavioral work has identified amplitude as a good summary of the entire pleasure responses (Brielmann and Pelli, 2017; Brielmann et al., 2017).

To assess how pleasure amplitude changes with overall rating and duration, we ran a 3 × 3 repeated measures ANOVA using the pleasure amplitude as the outcome variable. Greenhouse-Geisser corrections were applied to correct for violations of sphericity assumptions. Fig. 2D illustrates our results (see *Supplementary Materials* for the full ANOVA table of results). Both overall rating, $F(1.24, 84) = 133.24$, $p < 0.001$, $\eta_p^2 = 0.86$, and duration, $F(1.95, 84) = 15.31$, $p < 0.001$, $\eta_p^2 = 0.42$, affected pleasure amplitude. The main effects were accompanied by an interaction, $F(2.52, 84) = 33.24$, $p = 0.013$, $\eta_p^2 = 0.17$. Post-hoc pairwise comparisons with Bonferroni-adjustments showed that pleasure amplitude steadily increased from low to medium to high ratings for all durations (all $p < 0.001$, all $d \geq 0.91$). For all rating levels, pleasure amplitudes were higher for 5 compared to 1 s duration (all $p \leq 0.028$, all $d \geq 0.35$), but did not differ between 5 and 15 s (all $p \geq 0.134$). Pleasure amplitude was higher in 15 s than 1 s trials for both low- and high-rated images ($p \leq 0.006$ and $d \geq 0.45$ for both); this same tendency was also seen in medium-rated trials ($p = 0.066$, $d = 0.52$).

2.2. Aesthetic appreciation affects network-level responses

Average signal across the DMN was affected by aesthetic appreciation at all three image presentation durations. Responses from all three networks are plotted in Fig. 3, with the top row showing the network response to low-rated trials, and the bottom row showing the difference curves for high vs. low (green) and medium vs. low (blue). While trials of all three durations showed similar responses to aesthetic appreciation early in the trial – higher activity for high-than medium- or low-rated

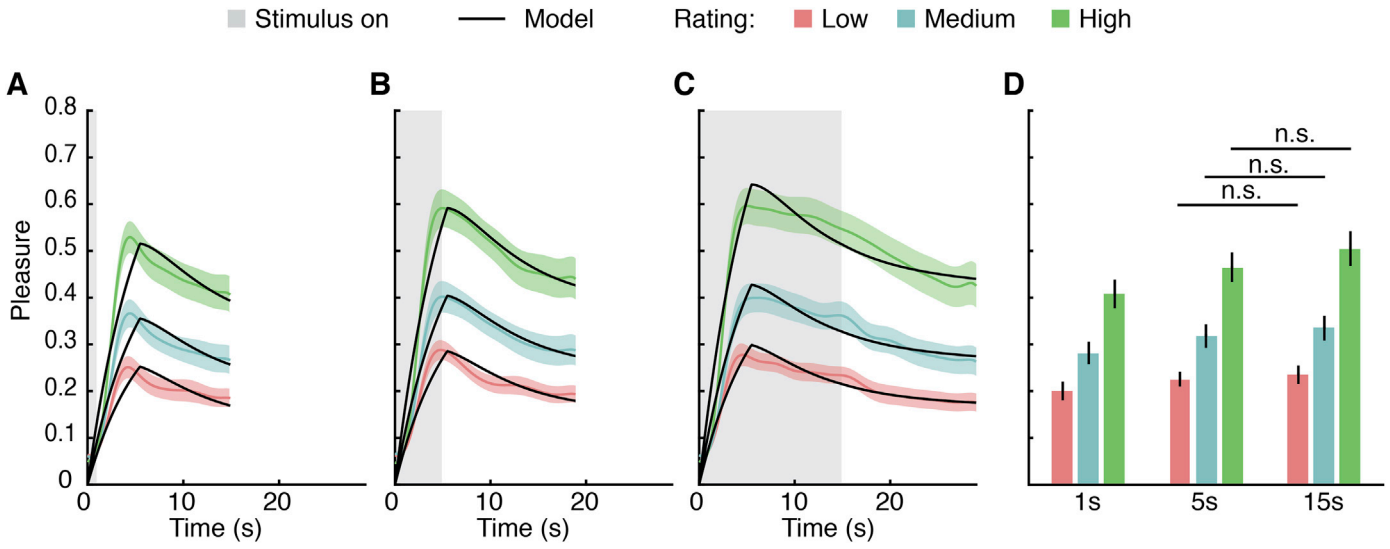

Fig. 2. Continuous pleasure responses. A-C) Average pleasure over time for high (green), medium (blue), and low (red) rated trials; colored shaded areas represent ±1 standard error of the mean (SEM). Black lines represent model fits. Gray shaded areas represent time windows during which the stimulus was present. Each panel shows data for one duration: 1 s (a), 5 s (b), and 15 s (c). D) Average pleasure amplitude r_{steady} per condition. Error bars represent ±SEM. All differences between ratings or durations are at least marginally significant, $p < 0.066$, unless otherwise indicated.

images – the underlying evolution of the DMN response differed depending on the duration of the stimulus (Fig. 3, first row). For 1-s trials [condition-by-time interaction, $F(14,336) = 1.96$, $p = 0.01$, $\eta_p^2 = 0.07$], at 6 s after image onset, high-rated images showed significantly greater activity than low ($p = 0.006$, $d = 0.83$) and medium-rated images ($p = 0.01$, $d = 0.56$; Fig. 3, second row). For these 1-s trials, the low response consisted of a slight dip followed by a small peak. For 5-s trials [$F(18,432) = 2.59$, $p < 0.001$, $\eta_p^2 = 0.09$] high-rated images showed significantly greater activity than low-rated images at onset ($p = 0.01$, $d = 0.66$), 6 s after image onset ($p < 0.001$, $d = 0.59$), and 8 s after image onset ($p = 0.04$, $d = 0.40$). For 5-s trials, there was initial suppression of the DMN by image presentation, replicating a pattern seen in a previous

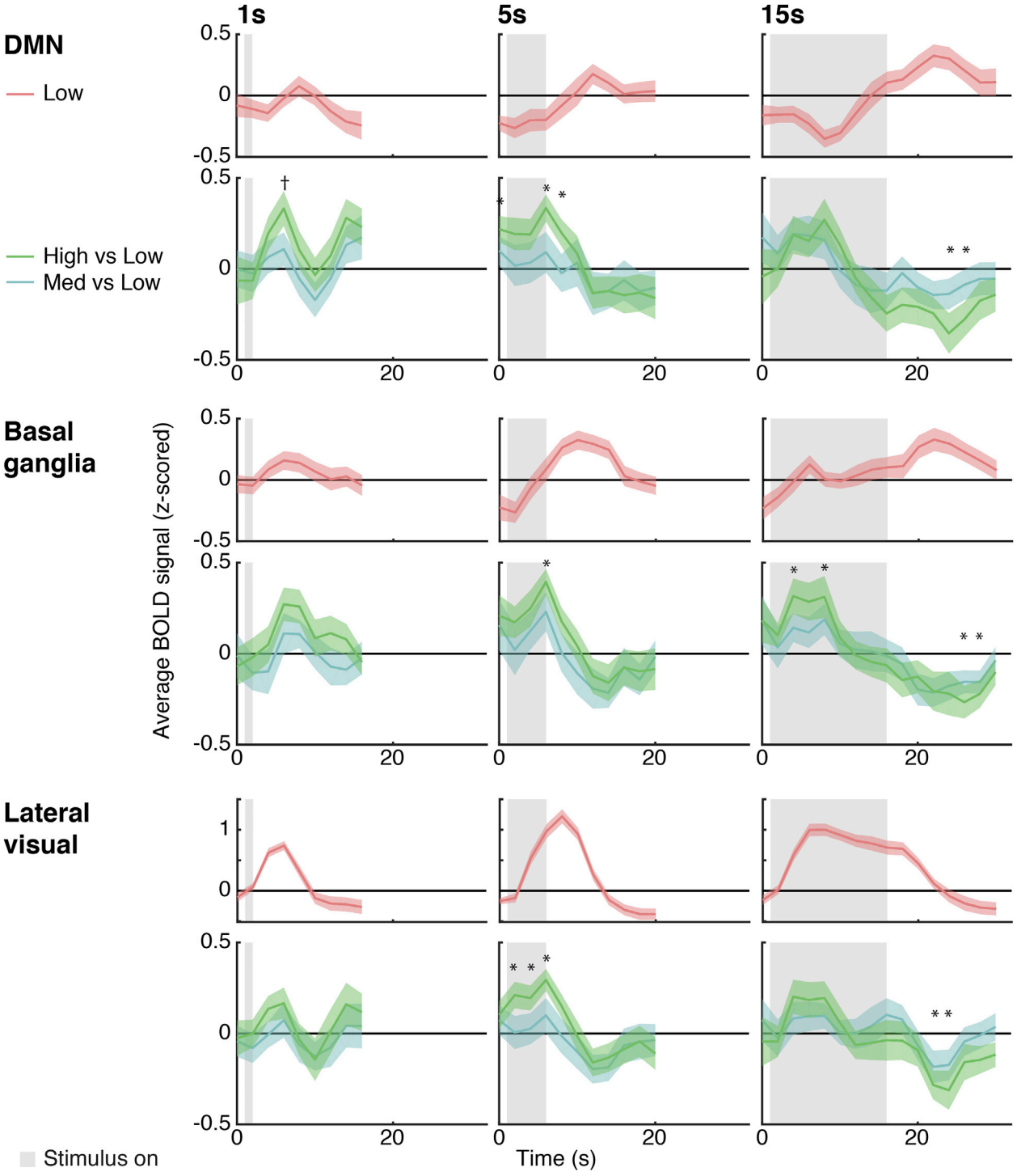

Fig. 3. Effects of aesthetic appreciation in large-scale brain networks. Trial-triggered average BOLD signal extracted from three large-scale brain networks: The default-mode network (DMN), the basal ganglia, and a lateral visual network (consisting of lateral occipitotemporal, ventral occipitotemporal, and parietal visual regions). For each network, the first row illustrates the response to low-rated trials (red), and the second row illustrates the *difference* between responses to high vs. low (green) and medium vs. low (blue) trials. Gray shading indicates image presentation (duration of 1, 5 or 15 s). The DMN and lateral visual networks were identified by correlating individual-participant ICA maps derived from a rest scan with published network maps (Smith et al., 2009). Color shaded areas indicate ±1 SEM. *Indicates significant differences between high and low trials. †Indicates significant differences between high trials vs. medium and low trials.

study (Vessel et al., 2013). For 15-s trials [$F(28,672) = 2.53$, $p < 0.001$, $\eta_p^2 = 0.09$], this suppression grew deeper and peaked later. In addition to the influence of aesthetic appreciation following the onset of the stimulus, the DMN also showed a delayed response that was most visible in the 15-s duration. Low-rated trials led to a positive BOLD response in the post-stimulus period that was greater than high-rated trials at 22 s ($p = 0.03$, $d = 0.50$), 24 s ($p = 0.01$, $d = 0.69$) and 26 s after image onset ($p = 0.02$, $d = 0.54$).

Similarly, we also observed influence of aesthetic appreciation in the basal ganglia after image onset (Fig. 3, fourth row), although the condition-by-time interaction did not reach significance in the one-second condition [$F(14,336) = 1.20$, $p = 0.27$, $\eta_p^2 = 0.04$]. However, for 5-s trials [$F(18,432) = 2.42$, $p < 0.001$, $\eta_p^2 = 0.09$], high-rated images showed significantly greater activity than low-rated images at 6 s ($p < 0.001$, $d = 0.39$). For 15-s trials [$F(28,672) = 2.82$, $p < 0.001$, $\eta_p^2 = 0.10$] high-rated images had significantly greater activity than low-rated images at 4 s ($p = 0.01$, $d = 0.64$), 6 s ($p = 0.03$, $d = 0.42$), and 8 s after stimulus onset ($p = 0.03$, $d = 0.70$). In contrast with the DMN responses, the underlying onset-responses in the basal ganglia were positive deflections from baseline regardless of duration (Fig. 3, third row). Interestingly, as seen in the DMN, in the 15-s condition a greater response was observed for low than high-rated images in the post-stimulus period [significant at 26 ($p = 0.02$, $d = 0.67$) and 28 s ($p = 0.02$, $d = 0.53$)].

The lateral visual network (composed of ventral and lateral occipito-temporal and inferior parietal regions) was modulated by aesthetic appreciation at the 5 and 15 s conditions, although this effect was confined to the initial image-onset response. One-second image duration trials [$F(14,336) = 0.97$, $p = 0.47$, $\eta_p^2 = 0.03$] showed no modulation by rating (Fig. 3, sixth row). For five-second trials [$F(18,432) = 2.82$, $p < 0.001$, $\eta_p^2 = 0.10$] high-rated images had significantly greater activity than low-rated images at 2 s ($p = 0.02$, $d = 0.63$), 4 s ($p = 0.02$, $d = 0.42$) and 6 s ($p < 0.001$, $d = 0.34$) after image onset. For fifteen-second trials [$F(28,672) = 1.96$, $p = 0.002$, $\eta_p^2 = 0.07$] low-rated images showed significantly greater activity than high-rated images at 22 s ($p = 0.004$, $d = 0.62$) and 24 s ($p = 0.02$, $d = 0.65$) after stimulus onset. These differences were superimposed on top of a strong visually-evoked response, which in the fifteen-second condition was composed of an initial response followed by a more sustained component with reduced amplitude.

2.3. Aesthetic appreciation affects DMN subregion responses

In order to investigate the relationship between aesthetic appreciation across all nodes of the DMN, we computed trial-triggered BOLD responses in five subregions: dmPFC, amPFC, vmPFC, PCC and IPL. Most subregions showed similar effects as the overall network, but there were differences in the strength and timing of the effect of aesthetic appreciation (Fig. 4) and the presence of suppression, which was strongest in the DMN "core" regions (PCC and amPFC) and the IPL.

Although there was a trend toward a significant relationship between dmPFC activity and aesthetic appreciation for 1-s [condition-by-time interaction $F(14,336) = 1.35$, $p = 0.17$, $\eta_p^2 = 0.05$], and 5-s [$F(18,432) = 1.68$, $p = 0.05$, $\eta_p^2 = 0.06$], the interaction was only significant for 15-s durations [$F(28,672) = 1.80$, $p < 0.001$, $\eta_p^2 = 0.07$]. High-rated images showed significantly less activity than low-rated images at 24 s ($p = 0.008$, $d = 0.69$), and 26 s ($p = 0.04$, $d = 0.50$; Fig. 4, top row).

The amPFC response also did not show significant relationships with aesthetic appreciation for 1-s [$F(14,336) = 1.69$, $p = 0.06$, $\eta_p^2 = 0.06$] or 5-s trials [$F(18,432) = 0.93$, $p = 0.53$, $\eta_p^2 = 0.03$], but was significant for 15-s trials [$F(28,672) = 1.70$, $p = 0.01$, $\eta_p^2 = 0.07$]. High-rated trials had significantly greater activity than low-rated trials at 8 s ($p = 0.04$, $d = 0.70$) and low-rated trials had significantly greater activity than high-rated trials at 26 s ($p = 0.03$, $d = 0.51$; Fig. 4, second row).

The vmPFC did not show a significant relationship with aesthetic appreciation at 1-s [$F(14,336) = 1.62$, $p = 0.07$, $\eta_p^2 = 0.06$] 5-s [$F(18,432) = 0.98$, $p = 0.47$, $\eta_p^2 = 0.04$] or 15-s trials [$F(28,672) = 2.11$, $p = 0.30$, $\eta_p^2 = 0.04$; Fig. 4, third row).

The PCC response did not show a significant relationship with aesthetic appeal for 1-s trials [$F(14,336) = 1.68$, $p = 0.06$, $\eta_p^2 = 0.06$] (Fig. 4, fourth row), but did show a significant relationship with aesthetic appreciation for 5-s trials [$F(18,432) = 2.48$, $p < 0.001$, $\eta_p^2 = 0.09$] at 6 s (high vs. low $p = 0.001$, $d = 0.78$). Additionally, the PCC showed lower signal for high-rated trials at 18 s post-stimulus onset in the 15-s duration [$F(28,672) = 2.11$, $p < 0.001$, $\eta_p^2 = 0.08$; high vs. low: $p = 0.02$, $d = 0.68$; high vs. medium $p = 0.01$, $d = 0.54$].

The IPL response showed a significant relationship with aesthetic appeal for 1-s trials [$F(14,336) = 1.95$, $p = 0.02$, $\eta_p^2 = 0.07$] (Fig. 4, bottom row). At 6 s after image onset there was a significant difference between high- and low-rated trials ($p = 0.04$, $d = 0.30$). There was also a significant effect for 5-s trials [$F(18,432) = 1.75$, $p = 0.02$, $\eta_p^2 = 0.06$], although none of the pairwise comparisons survived corrections for multiple comparisons. Finally, there was a significant relationship with aesthetic appeal for 15-s trials [$F(28,672) = 1.89$, $p = 0.003$, $\eta_p^2 = 0.07$]; there were significant differences between high- and low-rated trials at 16 s ($p = 0.006$, $d = 0.74$), 24 s ($p = 0.03$, $d = 0.63$), and 26 s ($p = 0.02$, $d = 0.58$) after image onset.

2.4. Aesthetic appreciation affects basal ganglia subregion responses

Sensitivity to aesthetic appreciation in the basal ganglia has been variously reported in a number of different regions, including the caudate (Ishizu and Zeki, 2011; Vartanian and Goel, 2004) and the nucleus accumbens/ventral striatum (Kim et al., 2007; Lacey et al., 2011). We extracted timecourses from four basal ganglia subregions (caudate, nucleus accumbens, putamen, pallidum) to compare the timecourses in these structures (Fig. 5).

The caudate did not show a significant relationship to aesthetic appreciation for 1-s trials [$F(14,336) = 0.68$, $p = 0.79$, $\eta_p^2 = 0.02$], but did show an early relationship with aesthetic appreciation for both the 5-s and 15-s trials (Fig. 5 top row). For 5-s trials [$F(18,432) = 2.68$, $p < 0.001$, $\eta_p^2 = 0.10$], high-rated images showed significantly greater activity than low-rated images at 6 s ($p < 0.001$, $d = 0.96$) and 8 s ($p = 0.003$, $d = 0.59$). For 15-s trials [$F(28,672) = 2.64$, $p < 0.001$, $\eta_p^2 = 0.09$], low-rated images had significantly less activity than high ($p = 0.005$, $d = 0.68$) and medium-rated images ($p = 0.04$, $d = 0.53$) at 4 s, and low-rated trails had significantly less activity than high-rated trials at 8 s ($p = 0.02$, $d = 0.76$). Additionally, low-rated trials had significantly more activity than high-rated trials at 26 s ($p = 0.02$, $d = 0.66$) and 28 s ($p = 0.02$, $d = 0.63$).

The putamen also showed no significant relationship to aesthetic appreciation for 1-s trials [$F(14,336) = 1.05$, $p = 0.39$, $\eta_p^2 = 0.04$], but early modulation by aesthetic appreciation for the 5-s duration [$F(18,432) = 1.79$, $p = 0.02$, $\eta_p^2 = 0.06$], at 6 s (high vs. low $p = 0.06$, $d = 0.57$) and for the 15-s duration [$F(28,672) = 2.69$, $p < 0.001$, $\eta_p^2 = 0.10$] at 4 s (high vs. low $p = 0.01$, $d = 0.54$) and 6 s (high vs. low $p = 0.03$, $d = 0.60$).

The response in the pallidum was not affected by aesthetic appreciation at the 1-s [$F(14,336) = 1.50$, $p = 0.10$, $\eta_p^2 = 0.05$] or 5-s durations [$F(18,432) = 1.21$, $p = 0.24$, $\eta_p^2 = 0.04$], and was only affected by aesthetic appreciation late in the trial for the 15-s duration [$F(28,672) = 1.81$, $p = 0.006$, $\eta_p^2 = 0.07$], at 24 s post-stimulus onset (low vs. medium $p = 0.03$, $d = 0.52$).

The nucleus accumbens also showed a relationship to aesthetic appreciation in the early response of the 15-s duration (Fig. 5 bottom row), but unlike the caudate and putamen, this difference was riding on top of a suppression for low-rated trials (Fig. S2), similar to that observed in the DMN. There was no aesthetic appreciation modulation for 1-s trials [$F(14,336) = 1.21$, $p = 0.26$, $\eta_p^2 = 0.04$]. At the 5-s duration [$F(18,432) = 1.87$, $p = 0.01$, $\eta_p^2 = 0.07$], high trials showed significantly greater activity than low trials at 6 s ($p = 0.005$, $d = 0.70$). For the 15-s duration [$F(28,672) = 1.82$, $p = 0.005$, $\eta_p^2 = 0.07$], there was significant

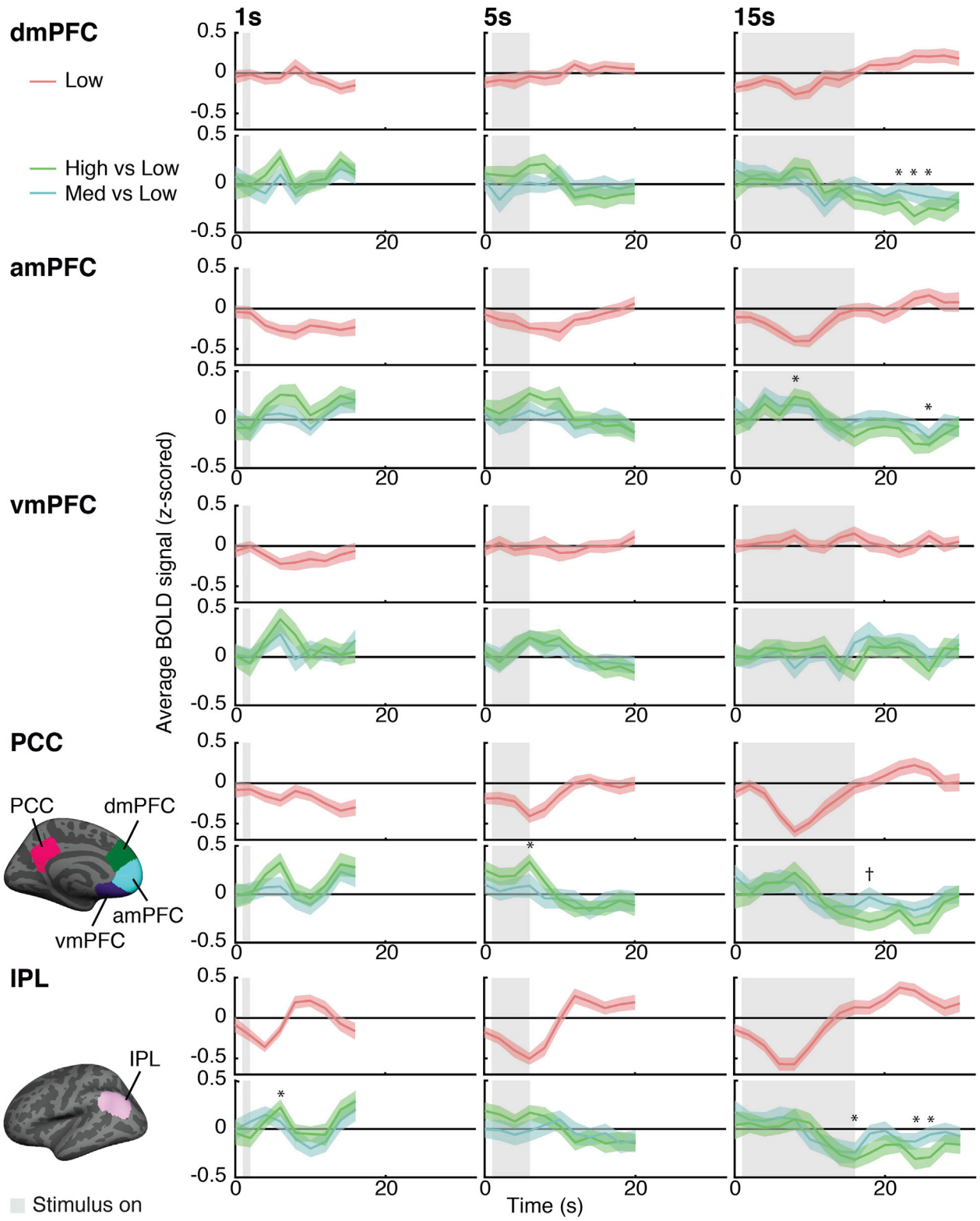

Fig. 4. Differential sensitivity in subregions of the DMN to aesthetic appreciation. For each region, the first row illustrates the response to low-rated trials (red), and the second row illustrates the *difference* between responses to high vs. low (green) and medium vs. low (blue) trials. Gray shading indicates image presentation (duration of 1, 5 or 15 s). Regions were extracted by combining individual-participant DMN maps with subregion masks defined in a common (Freesurfer fsaverage) surface space. Color shaded areas indicate ±1 SEM. *Indicates significant differences between high and low trials. †Indicates significant differences between high trials vs. medium and low trials.

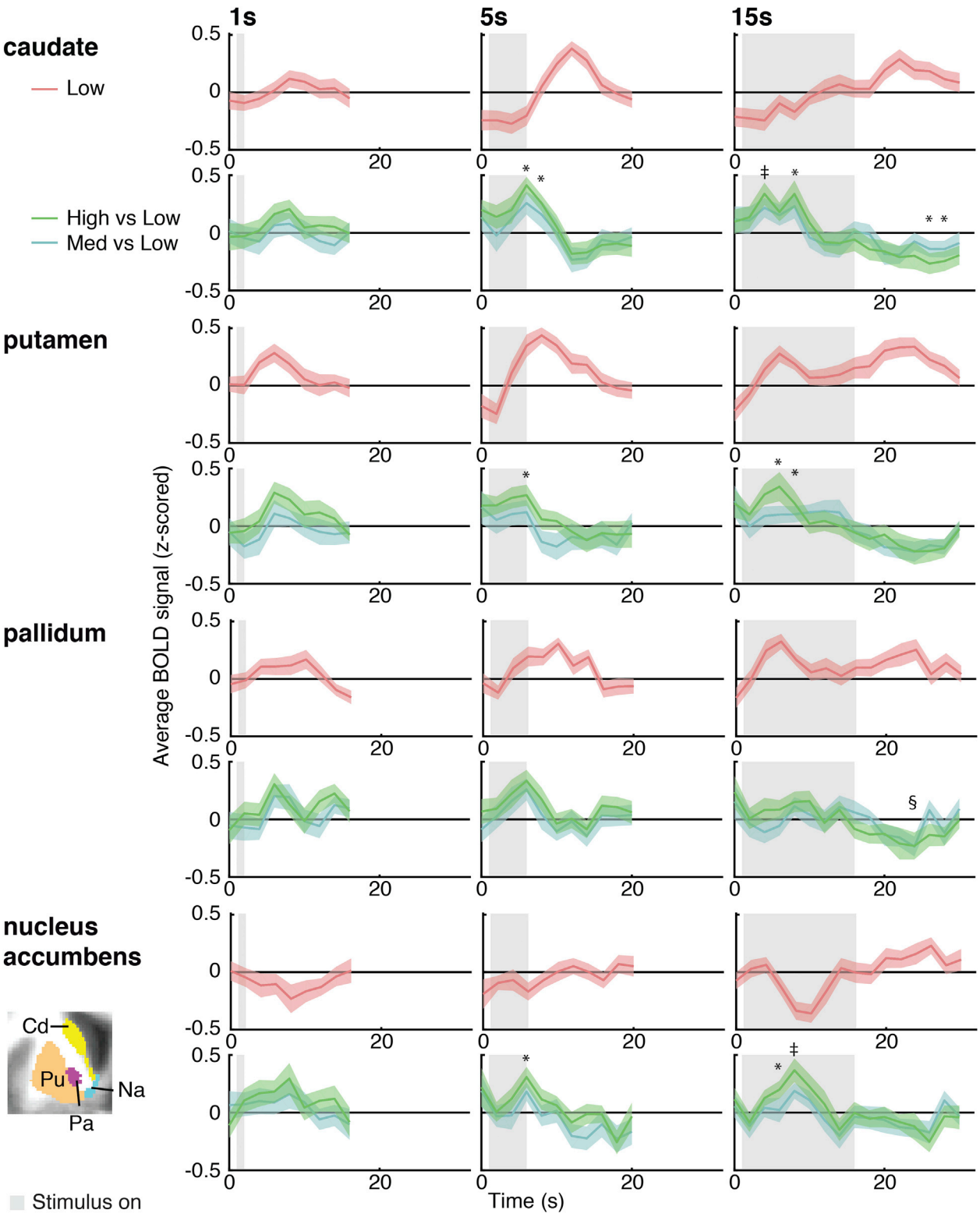

Fig. 5. Differential sensitivity of basal-ganglia subregions to aesthetic appreciation. For each region, the first row illustrates the response to low-rated trials (red), and the second row illustrates the *difference* between responses to high vs. low (green) and medium vs. low (blue) trials. Gray shading indicates image presentation (duration of 1, 5 or 15 s). ROIs were created from an automatic volumetric segmentation of individual participant high-resolution T1 scans (Freesurfer aseg). Color shaded areas indicate ±1 SEM. *Indicates significant differences between high and low trials. †Indicates significant differences between high trials vs. medium and low trials. ‡Indicates significant differences between low vs. high and medium trials. §Indicates significant differences between low and medium trials.

aesthetic appreciation modulation at 6 s (high vs. low, $p = 0.04$, $d = 0.54$) and 8 s (high vs. low, $p = 0.004$, $d = 0.86$; med vs. low, $p = 0.02$, $d = 0.73$).

3. Discussion

We found that activity in the DMN, a brain network hypothesized to support internally directed mentation (Buckner et al., 2008), responded to aesthetically pleasing art regardless of how long the art was viewed. With non-appealing images, suppression of the DMN increased for longer presentation durations. Unlike behavioral ratings of continuous pleasure, the DMN response did not linger after the image disappeared; rather, the DMN was transiently modulated by aesthetic appreciation and also "disengaged" from ongoing visual stimulation after about ten seconds (during 15 s low- and medium-rated trials), which may reflect the participant's return to stimulus-independent thought.

3.1. Felt pleasure corresponds with aesthetic appeal

Behaviorally, our findings replicate prior work indicating that continuous ratings of pleasure linger following aesthetic experiences (Brielmann and Pelli, 2017; Brielmann et al., 2017). While in the present study participants made continuous ratings using a squeezeball (in order to provide haptic feedback), prior work has used other response modalities, such as finger spread on the surface of a touchscreen. Despite these differences in response modality, our behavioral responses were well-fit by this prior model based on finger-spread responses (Brielmann and Pelli, 2017). Additionally, our results indicate that pleasure is relatively independent of stimulus duration beyond the initial few seconds: While the amplitude of continuous pleasure was higher for five than one-second stimuli, there were no differences between five and fifteen-second stimuli.

Behaviorally, we also found close correspondence between the continuous and overall ratings. At all three durations, 'high,' 'medium',' and 'low' rated trials, as defined by the overall rating, were all well modeled by a single function that differed only in the R_{steady} parameter, which decreased across the three rating levels and also showed some sensitivity to duration. Similarly, there was a strong correlation between the peak of the continuous rating and the overall rating ($R = 0.69$). This corresponds with previous work using music, which has indicated that the peak of a continuous rating is highly predictive of an overall, summative rating (Rozin et al., 2004; Schafer et al., 2014), and that ratings made early in a piece tend to correspond with those made at the end (Belfi et al., 2018a).

It is important to note that while our prior behavioral work found a strong correspondence between felt pleasure and beauty (Brielmann and Pelli, 2017; Brielmann et al., 2017), it was not clear *a priori* that such a simple relationship would be observed in this experiment, as the overall and continuous ratings were designed to measure different constructs: The overall rating was focused on aesthetic appreciation, specifically, how much a viewer felt "moved" by the art, while the continuous ratings were of felt pleasure. While feelings of "being moved" frequently contain both positive and negative emotions (Menninghaus et al., 2015), the influence of such emotions on the participant's overall emotional state may differ based on the context. In an aesthetic context, feelings of being moved are typically experienced as intensely pleasurable, even when driven by negatively-valenced emotions (Menninghaus et al., 2017a,b). Similarly, there is substantial work indicating the strong enjoyment and feelings of pleasure in response to negatively-valenced music (Eerola et al., 2016; Eerola et al., 2017; Kawakami et al., 2013).

Additionally, it is important to note that aesthetic experience is a complex and multi-dimensional experience, likely involving cognitive processes including visual imagery (Starr, 2013) and autobiographical memory (Belfi et al., 2016a). However, here we decided to focus on feelings of pleasure, as this has been identified as one of the most critical and necessary components of aesthetic experience (Brielmann and Pelli, 2017). Assessing this singular dimension does not rule out the possibility that aesthetic pleasure involves other components. However, from prior work it appears that judgments such as liking, beauty, and being moved tend to engage similar cognitive processes. For example, such judgments are highly correlated and have often been averaged together into a single rating to assess overall aesthetic appeal (Kraxenberger and Menninghaus, 2017; Ludtke et al., 2014; Menninghaus et al., 2017a,b).

Here, our results suggest that the peak of continuous felt pleasure is strongly related to an overall judgment of the aesthetic appreciation of an artwork. Prior work in other domains has indicated that metrics besides the peak may be more closely related to an overall rating (e.g., the peak-end rule; Do et al., 2008; Kahneman, 2000a). It may be the case that ratings of artworks differ from other domains. However, to fully understand the relationship between online, continuous ratings and a post-hoc summative rating, more research is needed. One consequence of this tight relationship between the continuous overall ratings seen here is that there was little variance in the continuous ratings that could be related to the BOLD signal, after accounting for the overall rating.

3.2. Aesthetically moving artworks engage the DMN

BOLD signal in the DMN reflected aesthetic appreciation at all three image durations. This response developed early (observable in the BOLD signal within 4–8 s after image onset) but was not sustained throughout the image presentation for the longest duration. Thus, the effect of aesthetic appreciation on DMN signal was largely transient and tied to the onset of the image. Indeed, the effect of aesthetic appeal even flipped direction after this initial response, with low-rated artworks correlated with higher signal late in the 5-s and 15-s conditions. Note that although the effect of aesthetic appeal was detected at a later timepoint in 15-s trials compared to the 1-s and 5-s trials, it is unclear whether this reflects a true delay for longer image presentation or possibly a temporally extended response to aesthetic appreciation for longer images.

The DMN response during 5-s trials showed a suppression for low- and medium-rated trials that was not present for high-rated trials. Although we were unable to detect specific evidence for a nonlinear response, this pattern is qualitatively similar to the "step-like" response reported in Vessel et al. (2012), in which they hypothesized that this pattern reflected a release from suppression in the DMN only for strongly aesthetically pleasing stimuli (Vessel et al., 2013). The current experiment sheds light on the nature of this suppression: Inspection of all three durations revealed that the BOLD suppression for low- and medium-rated trials grew longer with longer image duration, from only a few seconds (if at all) following 1-s presentations to more than 10 s at the longest duration (15 s). The influence of aesthetic appreciation, which was remarkably consistent across image duration, therefore appeared as *activation* following short duration stimuli, but as *less suppression* following long duration stimuli.

Analyses of five subregions of the DMN illustrated heterogeneity across the network. Modulation by aesthetic appreciation was observed in the amPFC and PCC, the 'core' regions of the DMN (Andrews-Hanna et al., 2010) as well as in the IPL, but was less pronounced in vmPFC. Interestingly, signals from amPFC, PCC and IPL were also most strongly suppressed by longer image durations. This heterogeneity may reflect the fact that the subdivisions of the DMN have different connectivity (Braga and Leech, 2015; Bzdok et al., 2013, 2015; Uddin et al., 2009). While nodes of the DMN are sensitive to aesthetic appeal, more research is needed to understand how this information propagates across the network, and how it relates to differences in the functional properties of DMN subdivisions and the processes they support.

Overall, these results suggest an important role for the DMN in aesthetic processing. While additional research will be needed to better understand this role, it is likely that aesthetically pleasing images are both more evocative and lead to increased internal mentation. It is not the case, however, that the DMN response solely reflects increased

attention to high-rated artworks. If this were the case, one would expect that DMN responses to any artwork would be greater than to looking at a blank screen (the resting baseline), and would be positively modulated by aesthetic appeal. Indeed, this is the pattern that was observed in both the lateral visual network and in the frontoparietal control network (FP; see Fig. S4). Alternatively, the broader DMN literature would suggest that it is typically anticorrelated with such "task-positive" networks, and is deactivated by externally-directed attentional effort (e.g. Fox et al., 2005). Our result shows that the DMN response to artwork, however, does not fit with this more typical pattern seen for attentionally demanding stimuli: If this were the case, one would predict *greater* deactivation for high-than low-rated images, not *less* deactivation.

The response we observe – anti-correlation with task-positive networks for low-rated stimuli but *positive* correlation for high-rated stimuli – likely reflects a change in large-scale network dynamics, and is consistent with a number of studies showing that the DMN is able to flexibly couple with putatively "task-positive" networks during certain tasks (Crittenden et al., 2015; Vatansever et al., 2015). We therefore suggest that increased activation of the DMN to high-rated artworks may instead reflect "engagement" with the stimulus, by which we mean that a person is "pulled in" to the stimulus, actively thinks about it, and chooses to continue mentally interacting with the stimulus (note that according to this definition it is possible to "attend" to a stimulus while not remaining engaged with it). How such engagement may relate to other hypothesized roles for the DMN during task execution, such as supporting episodic memory, working memory, prospective thinking and imagery, or the level of experiential detail (Sormaz et al., 2018) remains unclear. Such a role is consistent with the view that the DMN's anatomical position at the top of a cortical hierarchy permits it to flexibly integrate information over a variety of neural systems (Margulies et al., 2016). What may make its role in aesthetic appreciation noteworthy is the combination of external sensory input with internally self-generated information.

A potential concern is the initial offset below baseline in the DMN for the 5 s duration trials. This offset was likely an artifact resulting from an imbalance of the 1-back trial history of each condition and the relatively short 'jitter' time between trials. Such an imbalance is difficult to avoid when trials are sorted *post-hoc* on the basis of participant ratings and may be compounded by the large number of conditions (nine).

3.3. Disengagement of the DMN for non-pleasing artworks

The perceptual response, as gauged by the continuous pleasure ratings, was sustained through stimulus presentation and then slowly decayed. Yet none of the three networks we investigated showed sustained activation in the post-stimulus period. We did observe a late recovery of DMN signal (most apparent in dmPFC, PCC and IPL) at the longest image duration (15-s). This rebound peaked well after stimulus offset and was strongest in low-rated trials, with signal in high-rated trials showing little change until after stimulus offset. It was not coincident with a BOLD increase in the lateral visual network and was similar to the typical "anti-correlated" relationship observed between signal increases in DMN and decreases in sensory networks with stimulus offset (e.g., Fox et al., 2005) that correspond to a return to 'stimulus-independent thought' (Mason et al., 2007; Spreng and Grady, 2010).

Furthermore, the timing of this signal rebound did not reflect the dynamics of external visual stimulation, but rather the dynamics of the participant's internal states (high or low aesthetic appreciation followed by continued engagement or disengagement). BOLD responses in the DMN plotted as a function of time since image offset (Fig. 6) support this conclusion: During high-rated trials, image offset was followed by a return-to-baseline regardless of duration (red arrow), whereas for low- and medium-rated trials, the timing of the return-to-baseline was inconsistent across the three durations. Thus, on high-rated trials the DMN response tracked stimulus onset and offset, but for low-rated trials its stereotyped response was merely triggered by stimulus onset with a subsequent timecourse independent of stimulus duration.

It is possible that participants did not maintain their interest in the low- and medium-rated artworks for the entire 15-s duration, and that the DMN signal increase reflects a "disengagement" from the image and a return to stimulus independent thought, even though the image remained on the screen. This possibility suggests that whereas DMN activation for high-rated artworks reflects a simultaneous (and paradoxical) focus on both the "internal" and "external," a late DMN activation for low-rated stimuli reflects a return to purely "internal" focus. Future research is needed to better characterize this disengagement and test potential underlying mechanisms, such as repetition suppression in ventral visual regions (e.g. Turk-Browne et al., 2006) or competing (internal) sources of focus.

3.4. Response to aesthetic appreciation in both dorsal and ventral striatum

The pattern of response in the basal ganglia conforms to what is expected of regions sensitive to rewards of aesthetically pleasing images. The response was tied to image onset, sensitive to aesthetic appreciation, and only minimally affected by image duration.

The location and nature of modulation by rewarding stimulation within the basal ganglia is an unsettled issue. A large literature points to a role for the dorsal striatum (e.g. caudate, putamen) in the anticipation of reward and punishment (Delgado et al., 2003; Delgado et al., 2000) and to the ventral striatum (e.g. nucleus accumbens) in the actual experience of reward and computation of reward prediction error. A study using music (Salimpoor et al., 2011) found a pattern of activation consistent with this division. However, our previous study with visual artwork found a region straddling the dorsal and ventral striatum whose signal correlated with aesthetic pleasure (Vessel et al., 2012). A recent study of "chills" responses to poetry found the opposite: activation in the caudate at the start of a chill, and activation in the nucleus accumbens during the "pre-chill" period (Wassiliwizky et al., 2017). Additional evidence against the standard account comes from a patient study in which dorsal striatum damage negatively impacted stimulus-value learning but not action-value learning (Vo et al., 2014).

The responses of basal ganglia, while quite similar in some respects to

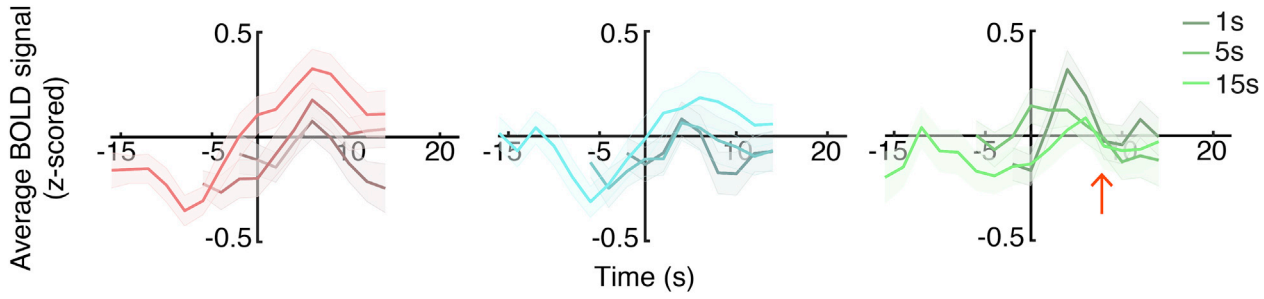

Fig. 6. DMN shows a response locked to stimulus offset for only high-rated trials. DMN responses aligned by offset for low (left) medium (middle) and high-rated trials (right). Darkest colors depict 1 s trials, medium colors depict 5 s trials, and brightest colors depict 15 s trials. Red arrow depicts timepoint at which BOLD signal returns to baseline simultaneously for all three trial durations; this is not present in low and medium-rated trials.

the DMN, differed in other ways. First, the relationship to the baseline differed; at the 5 and 15 s presentation durations, DMN responses were negative for low- and medium-preferred images, whereas basal ganglia responses were positive (note that the nucleus accumbens also exhibited signal decreases). Second, inspection of response amplitudes in the basal ganglia appear to increase from low-to medium-, and again from medium-to high-rated trials, whereas the response in the DMN, particularly for 1-s and 5-s presentations, shows little difference between medium- and low-rated trials. Again, while this dataset is unable to statistically distinguish between linear and nonlinear responses, this pattern is qualitatively consistent with the distinction between "linear" and "step-like" responses reported in Vessel et al. (2012). Such a difference could emerge from a two-stage process in which (1) the basal ganglia compute a linear representation of the hedonic value of the stimulus, and (2) if that value exceeds a threshold, the DMN is released from suppression, supporting inwardly oriented processing coincident with ongoing externally oriented sensory processing.

3.5. Sensitivity to aesthetic appreciation in higher-level visual regions

Modulation of the lateral visual network by aesthetic appreciation was observed during the 5-s and 15-s duration trials and did not persist beyond the initial transient response, in a manner strikingly similar to that observed for the DMN and basal ganglia. This is consistent with previous reports of sensitivity to aesthetic appreciation in higher-level regions of the ventral visual pathway (Cattaneo et al., 2015; Jacobsen et al., 2006; Kim et al., 2007; Vartanian and Goel, 2004; Yue et al., 2007). It is unclear if this sensitivity to aesthetic appreciation in a perceptual pathway is a bottom-up or top-down effect: In the 5-s duration, the difference between high- and low-rated stimuli in the lateral visual network was statistically detectible sooner than the difference in the basal-ganglia, but this order was reversed in the 15-s duration.

It is important to mention that the results seen here are unlikely to be due to differences in visual features among the various stimuli. One consistent finding in the field of empirical aesthetics is that individuals tend to show high variability in their preferences; that is, individuals do not agree on what they find aesthetically pleasing in images, music, or poetry (Belfi et al., 2018b; Vessel and Rubin, 2010; Vessel et al., 2018). Due to this, it is unlikely in the present experiment that certain images appeared consistently as high- or low-rated. To formally assess this, we calculated the intraclass correlation coefficient (ICC) from single measures for the overall ratings using the ICC(2,1) consistency measure (McGraw and Wong, 1996). This analysis revealed low agreement among raters (ICC value = 0.10, 95% CI: [0.07, 0.15]). This indicates that images were not systematically rated as high or low, indicating that our results are unlikely the result of differences in visual features between the conditions.

4. Conclusions

Aesthetically pleasing interactions with visual artworks dynamically engage perceptual, reward, and DMN networks, resulting in both transient and sustained changes in network activation. By varying the duration of the art image, we distinguished stimulus-driven from intrinsic dynamics. Stimulus-driven dynamics ended shortly after stimulus offset and included visual responses in higher-level visual regions and reward responses in the basal ganglia and DMN. Intrinsic dynamics included suppression of the DMN for longer stimuli (i.e., 15 s), time-locked changes in the DMN for offset of high-rated artworks, and possible "disengagement" of the DMN for low-rated stimuli. These dynamics suggest that the DMN tracks the participant's internal state during continued engagement with aesthetically pleasing experiences, as well as during disengagement from non-pleasing stimuli.

Although there remains much to be learned about how the brain supports aesthetic experience, these results support a general picture of visual aesthetic experience that involves the complex interaction of neural systems for sensation, understanding and reward (Chatterjee and Vartanian, 2014; Leder and Nadal, 2014). We suggest that the DMN is part of a system that engages in top-down sense-making (and imagery) in interaction with the bottom-up flow of information through sensory hierarchies. This interplay, a form of mental "free play," has the potential to bring about complex emotional responses and "pleasure through understanding" (Biederman and Vessel, 2006) at multiple levels of analysis, from the purely formal to the highly conceptual and personal, along with subsequent activation of reward systems. Experiences that involve the extended interplay of bottom-up and top-down information, resulting in a continued, deepening engagement with perceptual input, are experienced as more aesthetically appealing.

Conflicts of interest

The authors declare no competing financial interests.

Acknowledgements

We would like to acknowledge the following: Clay Curtis for suggestions on statistical analysis, Kat Markowski for help with fMRI data preprocessing, David Poeppel for help with project management, and Lauren Vale for help with squeezeball implementation. Funding was provided by the NYU Global Institute for Advanced Study.

Grateful acknowledgement is given for permission to reproduce the following artworks depicted in **Fig. 1**: *An Ecclesiastic*, c. 1874. Mariano José Maria Bernardo Fortuny y Carbo. Oil on panel. The Walters Art Museum, Bequest of William T. Walters. 37.150. *Seated African Woman*, 1860s. Henri Regnauld (French, 1843-181). Oil on fabric. The Cleveland Museum of Art, Bequest of Noah L. Butkin. 1980.280. *Flowers in a Glass*, c. 1606. Ambrosius Bosschaert the Elder (Dutch, 1573–1621). Oil on copper. The Cleveland Museum of Art. Gift of Carrie Moss Halle in memory of Salmon Portland Halle. 1960.108. *Hidden Fortress*, c. 1961. Al Held (USA, 1928–2005). Acrylic on canvas. Walker Art Center, Gift of T.B. Walker Foundation. 64.18 Art © Al Held Foundation/Licensed by VAGA, New York, NY.

Appendix A. Supplementary data

Supplementary data to this article can be found online at https://doi.org/10.1016/j.neuroimage.2018.12.017.

References

Andrews-Hanna, J.R., Reidler, J.S., Sepulcre, J., Poulin, R., Buckner, R.L., 2010. Functional-anatomic fractionation of the brain's default network. Neuron 65 (4), 550–562. https://doi.org/10.1016/j.neuron.2010.02.005.

Beaty, R.E., Benedek, M., Silvia, P.J., Schacter, D.L., 2016. Creative cognition and brain network dynamics. Trends Cognit. Sci. 20 (2), 87–95. https://doi.org/10.1016/j.tics.2015.10.004.

Beckmann, C.F., Noble, J.A., Smith, S.M., 2001. Investigating the intrinsic dimensionality of fMRI data for ICA. In: Seventh International Conference on Functional Mapping of the Human Brain.

Belfi, A.M., Karlan, B., Tranel, D., 2016. Music evokes vivid autobiographical memories. Memory 24, 979–989.

Belfi, A.M., Kasdan, A., Rowland, J., Vessel, E.A., Starr, G.G., Poeppel, D., 2018a. Rapid timing of musical aesthetic judgments. J. Exp. Psychol. Gen. 147 (10), 1531–1543. https://doi.org/10.1037/xge0000474.

Belfi, A.M., Vessel, E.A., Starr, G.G., 2018b. Individual ratings of vividness predict aesthetic appeal in poetry. Psychol. Aesthet. Creat. Arts 12 (3) , 341–350. https://doi.org/10.1037/aca0000153.

Biederman, I., Vessel, E.A., 2006. Perceptual pleasure and the brain: A novel theory explains why the brain craves information and seeks it through the senses. Am. Sci. 94 (3), 247–253.

Bohrn, I.C., Altmann, U., Lubrich, O., Menninghaus, W., Jacobs, A.M., 2013. When we like what we know - A parametric fMRI analysis of beauty and familiarity. Brain Lang. 124, 1–8. https://doi.org/10.1016/j.bandl.2012.10.003.

Braga, R.M., Leech, R., 2015. Echoes of the brain: Local-scale representation of whole-brain functional networks within transmodal cortex. Neuroscientist 21 (5), 540–551. https://doi.org/10.1177/1073858415585730.

Brainard, D.H., 1997. The psychophysics toolbox. Spatial Vis. 10, 433–436.

Brieber, D., Nadal, M., Leder, H., Rosenberg, R., 2014. Art in time and space: Context modulates the relation between art experience and viewing time. PLoS One 9 (6), 1–8. https://doi.org/10.1371/journal.pone.0099019.
Brielmann, A.A., Pelli, D.G., 2017. Beauty requires thought. Curr. Biol. 1–8. https://doi.org/10.1016/j.cub.2017.04.018.
Brielmann, A.A., Vale, L., Pelli, D.G., 2017. Beauty at a glance. The feeling of beauty and the amplitude of pleasure are independent of stimulus duration. J. Vis. 17, 1–12. https://doi.org/10.1167/17.14.9 (14):9.
Buckner, R.L., Andrews-Hanna, J.R., Schacter, D.L., 2008. The brain's default network: Anatomy, function, and relevance to disease. Ann. N. Y. Acad. Sci. 1124, 1–38. https://doi.org/10.1196/annals.1440.011.
Burunat, I., Alluri, V., Toiviainen, P., Numminen, J., Brattico, E., 2014. Dynamics of brain activity underlying working memory for music in a naturalistic condition. Cortex 57 (M), 254–269. https://doi.org/10.1016/j.cortex.2014.04.012.
Bzdok, D., Heeger, A., Langner, R., Laird, A.R., Fox, P.T., Palomero-Gallagher, N., et al., 2015. Subspecialization in the human posterior medial cortex. Neuroimage 106, 55–71. https://doi.org/10.1016/j.neuroimage.2014.11.009.
Bzdok, D., Langner, R., Schilbach, L., Jakobs, O., Roski, C., Caspers, S., et al., 2013. Characterization of the temporo-parietal junction by combining data-driven parcellation, complementary connectivity analysis, and functional decoding. Neuroimage 81, 381–392. https://doi.org/10.1016/j.neuroimage.2013.05.046.
Cattaneo, Z., Lega, C., Ferrari, C., Vecchi, T., Cela-Conde, C.J., Silvanto, J., Nadal, M., 2015. The role of the lateral occipital cortex in aesthetic appreciation of representational and abstract paintings: A TMS study. Brain Cogn. 95, 44–53. https://doi.org/10.1016/j.bandc.2015.01.008.
Cela-Conde, C.J., Ayala, F.J., Munar, E., Maestú, F., Nadal, M., Capó, M.A., et al., 2009. Sex-related similarities and differences in the neural correlates of beauty. Proc. Natl. Acad. Sci. Unit. States Am. 106, 3847–3852. https://doi.org/10.1073/pnas.0900304106.
Cela-Conde, C.J., García-Prieto, J., Ramasco, J.J., Mirasso, C.R., Bajo, R., Munar, E., 2013. Dynamics of brain networks in the aesthetic appreciation. Proc. Natl. Acad. Sci. Unit. States Am. 110, 10454–10461. https://doi.org/10.1073/pnas.1302855110.
Chatterjee, A., 2004. Prospects for a cognitive neuroscience of visual aesthetics. Bull. Psychol. Arts 4, 56–60. https://doi.org/10.1017/S0140525X00040607.
Chatterjee, A., Vartanian, O., 2014. Neuroaesthetics. Trends Cognit. Sci. 18, 370–375. https://doi.org/10.1016/j.tics.2014.03.003.
Crittenden, B.M., Mitchell, D.J., Duncan, J., 2015. Recruitment of the default mode network during a demanding act of executive control. ELife 4, e06481. https://doi.org/10.7554/eLife.06481.001.
Cutting, J.E., 2003. Gustave Caillebotte, French impressionism, and mere exposure. Psychonomic Bull. Rev.Rev. 10, 319–343.
de Tommaso, M., Pecoraro, C., Sardaro, M., Serpino, C., Lancioni, G., Livrea, P., 2008. Influence of aesthetic perception on visual event-related potentials. Conscious. Cognit. 17, 933–945. https://doi.org/10.1016/j.concog.2007.09.003.
Delgado, M.R., Locke, H.M., Stenger, V.A., Fiez, J.A., 2003. Dorsal striatum responses to reward and punishment: effects of valence and magnitude manipulations. Cognit. Affect Behav. Neurosci. 3 (1), 27–38. https://doi.org/10.3758/CABN.3.1.27.
Delgado, M.R., Nystrom, L.E., Fissell, C., Noll, D.C., Fiez, J.A., 2000. Tracking the hemodynamic responses to reward and punishment in the striatum. J. Neurophysiol. 84, 3072–3077. https://doi.org/10.1016/0166-2236(90)90107-l.
Desai, R.H., Choi, W., Lai, V.T., Henderson, J.M., 2016. Toward Semantics in the Wild: Activation to Manipulable Nouns in Naturalistic Reading. J. Neurosci. 36 (14), 4050–4055. https://doi.org/10.1523/JNEUROSCI.1480-15.2016.
Do, A.M., Rupert, A.V., Wolford, G., 2008. Evaluations of pleasurable experiences: the peak-end rule. Psychonomic Bull. Rev.Rev. 15, 96–98.
Eerola, T., Vuoskoski, J.K., Kautiainen, H., 2016. Being moved by unfamiliar sad music is associated with high empathy. Front. Psychol. 7 (SEP), 1–12. https://doi.org/10.3389/fpsyg.2016.01176.
Eerola, T., Vuoskoski, J.K., Peltola, H.R., Putkinen, V., Schäfer, K., 2017. An integrative review of the enjoyment of sadness associated with music. Phys. Life Rev. 1, 1–22. https://doi.org/10.1016/j.plrev.2017.11.016.
Fairhall, S.L., Ishai, A., 2008. Neural correlates of object indeterminacy in art compositions. Conscious. Cognit. 17 (3), 923–932. https://doi.org/10.1016/j.concog.2007.07.005.
Faul, F., Erdfelder, E., Lang, A.-G., Buchner, A., 2007. G*Power 3: A flexible statistical power analysis program for the social, behavioral, and biomedical sciences. Behav. Res. Methods 39, 175–191.
Flexas, A., Rossello, J., de Miguel, P., Nadal, M., Munar, E., 2014. Cognitive control and unusual decisions about beauty: An fMRI study. Front. Hum. Neurosci. 8, 1–9. https://doi.org/10.3389/fnhum.2014.00520.
Fox, M.D., Snyder, A.Z., Vincent, J.L., Corbetta, M., Van Essen, D.C., Raichle, M.E., 2005. The human brain is intrinsically organized into dynamic, anticorrelated functional networks. Proc. Natl. Acad. Sci. U. S. A 102 (27), 9673–9678. https://doi.org/10.1073/pnas.0504136102.
Huth, A.G., Heer, W. A. De, Griffiths, T.L., Theunissen, F.E., Jack, L., 2016. Natural speech reveals the semantic maps that tile human cerebral cortex. Nature 532 (7600), 453–458. https://doi.org/10.1038/nature17637.
Ishizu, T., Zeki, S., 2011. Toward a brain-based theory of beauty. PLoS One 6, e21852. https://doi.org/10.1371/journal.pone.0021852.
Jacobs, R.H.A.H., Renken, R., Cornelissen, F.W., 2012. Neural correlates of visual aesthetics - beauty as the coalescence of stimulus and internal state. PLoS One 7, e31248. https://doi.org/10.1371/journal.pone.0031248.
Jacobsen, T., Höfel, L., 2003. Descriptive and evaluative judgment processes: Behavioral and electrophysiological indices of processing symmetry and aesthetics. Cognit. Affect Behav. Neurosci. 3 (4), 289–299. https://doi.org/10.3758/CABN.3.4.289.
Jacobsen, T., Schubotz, R.I., Höfel, L., Cramon, D.Y.V., 2006. Brain correlates of aesthetic judgment of beauty. Neuroimage 29, 276–285. https://doi.org/10.1016/j.neuroimage.2005.07.010.
Kahneman, D., 2000a. Evaluation by Moments : Past and Future. In: Kahneman, D., Tversky, A. (Eds.), Choices, Values and Frames. Cambridge University Press, New York.
Kahneman, D., 2000b. Experienced utility of objective happiness: A moment-based approach. In: Kahneman, D., Tversky, A. (Eds.), Choices, Values and Frames. Cambridge University Press, New York.
Kawabata, H., Zeki, S., 2004. Neural correlates of beauty. J. Neurophysiol. 91, 1699–1705. https://doi.org/10.1152/jn.00696.2003.
Kawakami, A., Furukawa, K., Katahira, K., Okanoya, K., 2013. Sad music induces pleasant emotion. Front. Psychol. 4, 1–15. https://doi.org/10.3389/fpsyg.2013.00311.
Kim, H., Adolphs, R., O'Doherty, J., Shimojo, S., 2007. Temporal isolation of neural processes underlying face preference decisions. Proc. Natl. Acad. Sci. Unit. States Am. 104 (46), 18253–18258. https://doi.org/doi/10.1073/pnas.0711498105.
Kornysheva, K., Von Cramon, D.Y., Jacobsen, T., Schubotz, R.I., 2010. Tuning-in to the beat: Aesthetic appreciation of musical rhythms correlates with a premotor activity boost. Hum. Brain Mapp. 31, 48–64. https://doi.org/10.1002/hbm.20844.
Kraxenberger, M., Menninghaus, W., 2017. Affinity for poetry and aesthetic appreciation of joyful and sad poems. Front. Psychol. 7, 2051. https://doi.org/10.3389/fpsyg.2016.02051.
Lacey, S., Hagtvedt, H., Patrick, V.M., Anderson, A., Stilla, R., Deshpande, G., et al., 2011. Art for reward's sake: Visual art recruits the ventral striatum. Neuroimage 55, 420–433. https://doi.org/10.1016/j.neuroimage.2010.11.027.
Leder, H., Nadal, M., 2014. Ten years of a model of aesthetic appreciation and aesthetic judgments: The aesthetic episode - Developments and challenges in empirical aesthetics. Br. J. Psychol. 105, 443–464. https://doi.org/10.1111/bjop.12084.
Ludtke, J., Meyer-Sickendieck, B., Jacobs, A.M., 2014. Immersing in the stillness of an early morning: Testing the mood empathy hypothesis of poetry reception. Psychol. Aesthet. Creat. Arts 8, 363–377. https://doi.org/10.1037/a0036826.
Mallon, B., Redies, C., Hayn-Leichsenring, G.U., 2014. Beauty in abstract paintings: perceptual contrast and statistical properties. Front. Hum. Neurosci. 8, 161. https://doi.org/10.3389/fnhum.2014.00161.
Margulies, D.S., Ghosh, S.S., Goulas, A., Falkiewicz, M., Huntenburg, J.M., Langs, G., et al., 2016. Situating the default-mode network along a principal gradient of macroscale cortical organization. Proc. Natl. Acad. Sci. Unit. States Am., 201608282. https://doi.org/10.1073/pnas.1608282113.
Mason, M.F., Norton, M.I., Horn, J. D. Van, Wegner, D.M., Grafton, S.T., Macrae, C.N., et al., 2007. Wandering minds: The default network and stimulus-independent thought. Science 315, 393–395. https://doi.org/10.1126/science.1131295.
McGraw, K.O., Wong, S.P., 1996. Forming inferences about some intraclass correlations coefficients. Psychol. Methods 1, 390–390. https://doi.org/10.1037/1082-989X.1.4.390.
Menninghaus, W., Wagner, V., Hanich, J., Wassiliwizky, E., Jacobsen, T., Koelsch, S., 2017a. The Distancing-Embracing model of the enjoyment of negative emotions in art reception. Behav. Brain Sci. 40, E347. https://doi.org/10.1017/S0140525X17000309.
Menninghaus, W., Wagner, V., Hanich, J., Wassiliwizky, E., Kuehnast, M., Jacobsen, T., 2015. Towards a Psychological Construct of Being Moved. PLoS One 10 (6), e0128451. https://doi.org/10.1371/journal.pone.0128451.
Menninghaus, W., Wagner, V., Wassiliwizky, E., Jacobsen, T., Knoop, C.A., 2017b. The emotional and aesthetic powers of parallelistic diction. Poetics 63, 47–59. https://doi.org/10.1016/j.poetic.2016.12.001.
Minka, T., 2000. Automatic choice of dimensionality for PCA. Technical Report 514.
Müller, M., Höfel, L., Brattico, E., Jacobsen, T., 2010. Aesthetic judgments of music in experts and laypersons - An ERP study. Int. J. Psychophysiol. 76, 40–51. https://doi.org/10.1016/j.ijpsycho.2010.02.002.
Munar, E., Nadal, M., Castellanos, N.P., Flexas, A., Maestú, F., Mirasso, C., Cela-Conde, C.J., 2012. Aesthetic appreciation: Event-related field and time-frequency analyses. Front. Hum. Neurosci. 1–11. https://doi.org/10.3389/fnhum.2011.00185.
Nielsen, F., 1987. Musical tension and related concepts. In: Sebeok, T., Umiker-Sebeok, J. (Eds.), The Semiotic Web. Mouton de Gruyter, Berlin, pp. 491–513.
Park, J., Shimojo, E., Shimojo, S., 2010. Roles of familiarity and novelty in visual preference judgments are segregated across object categories. Proc. Natl. Acad. Sci. Unit. States Am. 107 (33), 14552–14555. https://doi.org/10.1073/pnas.1004374107.
Pearce, M.T., Zaidel, D.W., Vartanian, O., Skov, M., Leder, H., Chatterjee, A., Nadal, M., 2016. Neuroaesthetics: The Cognitive Neuroscience of Aesthetic Experience. Perspect. Psychol. Sci. 11 (2), 265–279. https://doi.org/10.1177/1745691615621274.
Pelli, D.G., 1997. The VideoToolbox software for visual psychophysics: transforming numbers into movies. Spatial Vis. 10, 437–442.
Pelowski, M., Markey, P.S., Forster, M., Gerger, G., Leder, H., 2017. Move me, astonish me… delight my eyes and brain: The Vienna Integrated Model of top–down and bottom–up processes in Art Perception (VIMAP) and corresponding affective, evaluative, and neurophysiological correlates. Phys. Life Rev. 80–125. https://doi.org/10.1016/j.plrev.2017.02.003.
Power, J.D., Barnes, K. a, Snyder, A.Z., Schlaggar, B.L., Petersen, S.E., 2012. Spurious but systematic correlations in functional connectivity MRI networks arise from subject motion. Neuroimage 59 (3), 2142–2154. https://doi.org/10.1016/j.neuroimage.2011.10.018.
Rozin, A., Rozin, P., Goldberg, E., 2004. The feeling of music past: How listeners remember musical affect. Music Percep. 4, 15–39. https://doi.org/10.1525/mp.2004.22.1.15.

Salimpoor, V.N., Benovoy, M., Larcher, K., Dagher, A., Zatorre, R.J., 2011. Anatomically distinct dopamine release during anticipation and experience of peak emotion to music. Nat. Neurosci. 14 (2), 257–262. https://doi.org/10.1038/nn.2726.

Schafer, T., Zimmermann, D., Sedlmeier, P., 2014. How we remember the emotional intensity of past musical experiences. Front. Psychol. 5, 1–10. https://doi.org/10.3389/fpsyg.2014.00911.

Shulman, G.L., Ollinger, J.M., Akbudak, E., Conturo, T.E., Snyder, A.Z., Petersen, S.E., Corbetta, M., 1999. Areas involved in encoding and applying directional expectations to moving objects. J. Neurosci. 19 (21), 9480–9496. https://doi.org/10.1523/JNEUROSCI.19-21-09480.1999.

Smith, S.M., Fox, P.T., Miller, K.L., Glahn, D.C., Fox, P.M., Mackay, C.E., et al., 2009. Correspondence of the brain's functional architecture during activation and rest. Proc. Natl. Acad. Sci. U. S. A 106 (31), 13040–13045. https://doi.org/10.1073/pnas.0905267106.

Sormaz, M., Murphy, C., Wang, H., Hymers, M., Karapanagiotidis, G., Margulies, D.S., et al., 2018. Default mode network can support the level of detail in experience during active task states. Proc. Natl. Acad. Sci. Unit. States Am. 115, 9318–9323. https://doi.org/10.1073/pnas.1721259115.

Spreng, R.N., Grady, C.L., 2010. Patterns of brain activity supporting autobiographical memory, prospection, and theory of mind, and their relationship to the default mode network. J. Cognit. Neurosci. 22, 1112–1123. https://doi.org/10.1162/jocn.2009.21282.

Spreng, R.N., Stevens, W.D., Chamberlain, J.P., Gilmore, A.W., Schacter, D.L., 2010. Default network activity, coupled with the frontoparietal control network, supports goal-directed cognition. Neuroimage 53, 303–317. https://doi.org/10.1016/j.neuroimage.2010.06.016.

Starr, G.G., 2013. Feeling beauty: The neuroscience of aesthetic experience. MIT Press, Cambridge, Massachussets.

Turk-Browne, N., Yi, D., Leber, A., Chun, M., 2006. Visual quality determines the direction of neural repetition effects. Cerebr. Cortex 17, 425–433. https://doi.org/10.1093/cercor/bhj159.

Uddin, L.Q., Kelly, A.M.C., Biswal, B.B., Castellanos, F.X., Milham, M.P., 2009. Functional connectivity of default mode network components: correlation, anticorrelation, and causality. Hum. Brain Mapp. 30, 625–637. https://doi.org/10.1002/hbm.20531.

Vartanian, O., Goel, V., 2004. Neuroanatomical correlates of aesthetic preference for paintings. Neuroreport 15, 487–491.

Vatansever, D., Menon, D.K., Manktelow, A.E., Shakian, B., Stamatakis, E., 2015. Default mode dynamics for global functional integration. J. Neurosci. 35, 15254–15262. https://doi.org/10.1523/JNEUROSCI.2135-15.2015.

Vessel, E.A., Rubin, N., 2010. Beauty and the beholder: highly individual taste for abstract, but not real-world images. J. Vis. 10 (2), 1–14. https://doi.org/10.1167/10.2.18.

Vessel, E.A., Maurer, N., Denker, A.H., Starr, G.G., 2018. Stronger shared taste for natural aesthetic domains than for artifacts of human culture. Cognition 179, 121–131. https://doi.org/10.1016/j.cognition.2018.06.009.

Vessel, E.A., Starr, G.G., Rubin, N., 2012. The brain on art: Intense aesthetic experience activates the default mode network. Front. Hum. Neurosci. 6, 66. https://doi.org/10.3389/fnhum.2012.00066.

Vessel, E.A., Starr, G.G., Rubin, N., 2013. Art reaches within: aesthetic experience, the self and the default mode network. Front. Neurosci. 7, 258. https://doi.org/10.3389/fnins.2013.00258.

Vo, K., Rutledge, R.B., Chatterjee, A., Kable, J.W., 2014. Dorsal striatum is necessary for stimulus-value but not action-value learning in humans. Brain 137, 3129–3135. https://doi.org/10.1093/brain/awu277.

Wassiliwizky, E., Koelsch, S., Wagner, V., Jacobsen, T., Menninghaus, W., 2017. The emotional power of poetry: neural circuitry, psychophysiology, compositional principles. Soc. Cognit. Affect Neurosci. 2017, 1–12. https://doi.org/10.1093/scan/nsx069.

Yue, X., Vessel, E.A., Biederman, I., 2007. The neural basis of scene preferences. Neuroreport 18 (6), 525–529. https://doi.org/10.1097/WNR.0b013e328091c1f9.